5B.1 Influence of Atmospheric Rivers on Long-Duration Freezing Rain Events in Eastern North America

Douglas K. Miller *[1]
University of North Carolina Asheville, Asheville, North Carolina

1. BACKGROUND

Although relatively rare, freezing rain events have significant societal impacts. The accumulation of ice on tree limbs and power lines causes widespread power outages that can result in serious health concerns (e.g., hypothermia) if the outages are long-lived. Also, ice accumulation on road and aircraft surfaces is responsible for casualties associated with accidents on roadways and for delays and cancellations of air traffic.

A schematic of the vertical profile of a textbook freezing rain scenario (Figure 1) shows a shallow layer of cold air resting next to the ground, with sub-freezing surfaces (e.g., roads and trees) residing in the layer. A mid-level layer having warm temperatures (warm nose) above the surface-based cold layer melts ice hydrometeors as they fall from the production layer above. The surface-based cold layer of air is deep enough to bring the melted ice to a super-cooled temperature, but not so deep as to freeze the droplets before coming in contact with the sub-freezing objects (e.g., roads, trees, power lines) on the ground below.

Freezing rain events are rare as the needed cold air layer next to the ground is difficult to initiate and maintain as it requires continual cold air advection by a nearby surface anticyclone to offset warming caused by latent heat release when the super-cooled water droplets freeze. It is also difficult to initiate and maintain the warm layer at mid-levels as it requires warm air advection by a nearby cyclone, circulating warm and humid air northward to offset the cooling of the environment caused by melting ice hydrometeors. Hence, the challenge of creating and maintaining a long-duration (LD) freezing rain event for northern domains is the continual movement of warm, humid air poleward and the continual equatorward movement of cold, dry air next to the ground is the challenge for southern domains.

Severe freezing rain events have large accumulations of ice. As summarized in Doswell et al. (1996), the total event precipitation accumulation of any event Is a combination of both the average precipitation rate of the event and the total event duration. Gyakum (2008) defines the precipitation rate (*P*) as

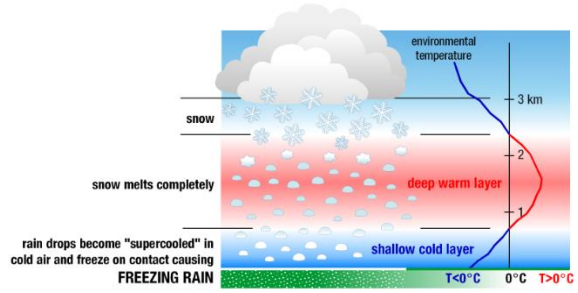

Figure 1. Freezing rain schematic showing a vertical temperature profile and the needed characteristics in the layers aloft to produce a coating of ice on surfaces in the cold layer of air adjacent to the ground (image link: https://www.nssl.noaa.gov/education/svrwx101/winter/types/img/freezingrain.png).

$$P = -\left(\frac{1}{g}\right)\int_{1000\ hPa}^{200\ hPa} \omega \left(\frac{dr_s}{dp}\right)_{ma} dp \qquad (1)$$

where *g* is gravity, the vertical integral extends from 1000 to 200 hPa, r_s is the saturation mixing ratio, and subscript '*ma*' represents the moist adiabat of the saturated air parcel. In subsequent discussions the vertical motion term of the integral in Eq. (1) will be referred to as the 'dynamic' term, while the term having the change of the saturation mixing ratio with height of the appropriate moist adiabat will be referred to as the 'thermodynamic' term.

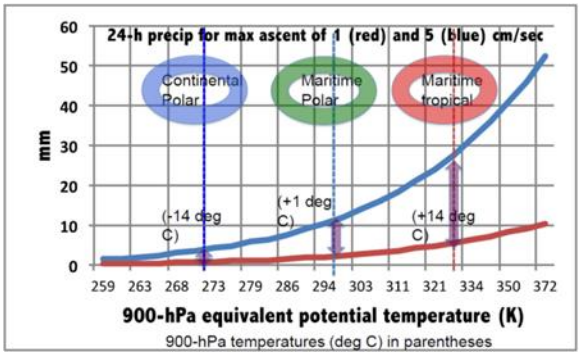

Figure 2. Twenty four-h precipitation (mm) plotted as a function of 900-hPa equivalent potential temperature and vertical motion (red curve; 1 cm s^{-1}, blue curve; 5 cm s^{-1}) from Gyakum (2016).

* *Corresponding author address:* Douglas K. Miller, Univ. of North Carolina Asheville, ATMS Department, CPO #2450, Asheville, NC 28804-8511;
e-mail: dmiller@unca.edu

Accumulated precipitation for a 24-h period (Figure 2) described in Gyakum (2016) shows the variability of precipitation as a function of different dynamic and thermodynamic forcings, calculated assuming the vertical motion profile to have a parabolic shape. The red and blue curves are accumulation results for the vertical motion profile peaking at 1 and 5 cm s^{-1}, respectively. Variation of equivalent potential temperature represents a shift in air mass type from continental polar air (left) to maritime tropical air (right), reflecting the impact of the thermodynamic term. The change in saturation mixing ratio with height is large for air masses having higher specific humidity. As a result, maritime tropical air masses have the potential of producing a large amount of precipitation given strong dynamical forcing compared to the lower humidity air masses. Also, for a given amount of dynamical forcing (following the red or blue curve in Fig. 2), a slight increase in maritime tropical humidity (referred to as 'intensity' in the discussion below) can yield significant increases in accumulated precipitation.

For forecast regions in the northern part of eastern North America, the transport of warm humid air poleward is challenging but necessary to create favorable conditions for freezing rain events (Figure 1). A logical large-scale feature bringing these conditions to northern regions is the atmospheric river (Figure 3). Atmospheric rivers are responsible for transporting vast amounts of water vapor from the tropics or sub-tropics, maritime tropical air masses, toward the poles, in a narrow corridor ahead of the surface cold front. This transport is focused in the lowest layer of the troposphere, occurring primarily within the layer between sea level and four kilometers. The purpose of this study is to examine a potential linkage between severe freezing rain events, assumed to be long-duration (LD) events, see McCray et al. (2019), and atmospheric rivers. The hypothesis is that severe freezing rain events can be traced to mid-latitude storms having an atmospheric river (AR).

2. METHODOLOGY

A parameter often used to flag mid-latitude storms having an AR is the integrated vapor transport (IVT [kg m^{-1} s^{-1}], Guan and Waliser; 2015), defined as

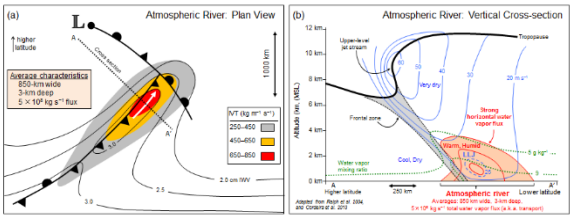

Figure 3. Schematics of the (a) horizontal and (b) vertical aspects of the atmospheric river (courtesy Glossary of Meteorology: http://glossary.ametsoc.org/wiki/Atmospheric_river).

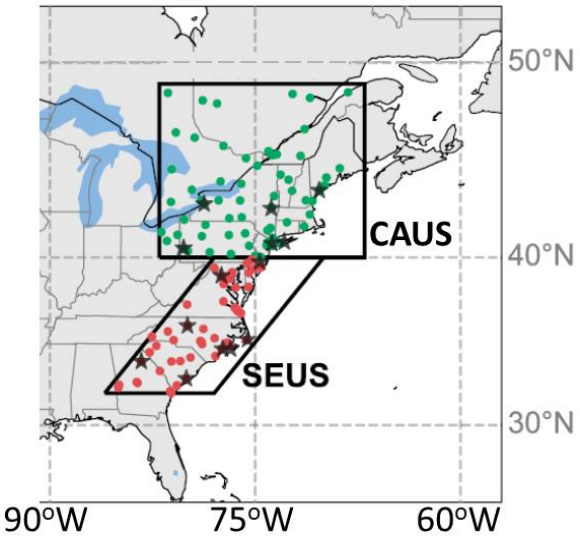

Figure 4. Study domains with dots showing locations of surface observation stations contributing to the freezing rain database of McCray et al. (2019). Modified version of Fig. 2 of McCray et al. (2019).

$$IVT = -\left(\frac{1}{g}\right)\int_{1000\ hPa}^{100\ hPa}(q\boldsymbol{V})\,dp \qquad (2)$$

where g is gravity, the vertical integral extends from 1000 to 100 hPa, q is the specific humidity, and $\boldsymbol{V}$ is the horizontal wind vector. The AR events database of Guan and Waliser (2015) is used in the study to investigate their influence on severe freezing rain events. The AR database was derived using meteorological fields of the Climate Forecast System Reanalysis (CFSR) six-hourly half-degree gridded dataset as input to compute IVT. IVT based on the 85th percentile specific to each season and grid cell and a fixed lower limit of 100 kg m^{-1} s^{-1} qualified as an AR, as long as its length exceeded 2000 km and its length-to-width ratio exceeded two. The AR database covers the 1 January 1979 through 31 December 2015 period (37 years).

The freezing rain database of McCray et al. (2019) is used in the study to define events in two study domains (Figure 4), a northern (CAUS) and southern (SEUS) domain located in eastern North America. The comparison of events to the presence of ARs is limited to the freezing rain seasons of 36 years (1980-2015), since the ARs database concludes with events in December 2015.

Freezing rain observations are binned in 6-h synoptic periods that correspond to the time resolution of the Guan and Waliser (2015) ARs database. A long-duration (LD) freezing rain event is defined in this study as an event having at least two consecutive 6-h synoptic periods in which at least one station in a given domain observes freezing rain. Following Miller et al. (2018), a freezing rain event concludes when a 6-h synoptic period has no reports of freezing rain.

3. RESULTS

Freezing rain season hours, shown in Figure 5, consist of the number of hours between the start of the first and the end of the final LD freezing rain event of each of the 36 cool seasons investigated in the study. It should be noted that ARs occurring only during these freezing rain seasons are examined in this study. Of note is the fact that the season length of the northern domain (CAUS) is nearly double that of the southern domain (SEUS).

Examination of the LD freezing rain events in both domains shows a significant number occurring in the northern domain (Figure 6, upper; blue) compared to those occurring in the southern domain (Figure 6, lower; blue). In either domain, a substantial fraction of the LD freezing rain events in both domains are influenced by ARs (compare orange to blue curve counts). This result is demonstrated in Table 1 showing totals over the 36-year study period. More than half of LD freezing rain events in the northern domain (56.7%) are associated with an AR, while these events tend to have longer duration (65.4%) than those events NOT associated with an AR. These fractions are not as large for the LD freezing rain events of the southern domain (count; 48.4% and hours; 50.9%, respectively).

Focusing on the VERY LONG LD freezing rain events, defined as events lasting 24-h or longer (Figure 7), the fraction of AR-influenced events for both the northern and southern populations increases markedly (Table 2). Of the 538 CAUS VERY LONG LD freezing rain events, 382 had an AR-influence (71.0%), a substantial increase of the original LD freezing rain fraction (56.7%). The hours associated with these events suggests they are skewed toward being quite long in duration (73.5%). Fractional increases for the southern domain are not as dramatic in terms of count (57.4% v. 48.4%) or event duration (56.0% v. 50.9%), but the same general observation holds, that AR-influenced freezing rain events tend toward being quite long-lived and, likely, severe.

Ranking the freezing rain events by the number of

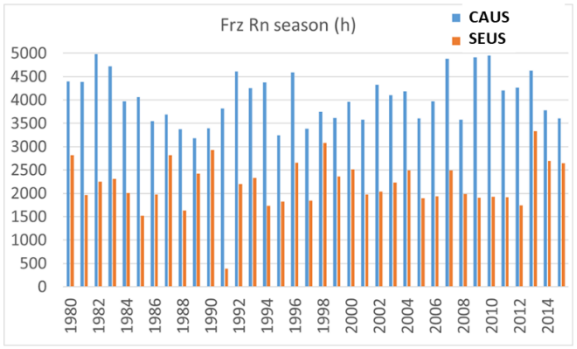

Figure 5. Freezing rain seasons (hours) for the northern (CAUS, blue) and southern (SEUS, orange) domains over the 36-year study period.

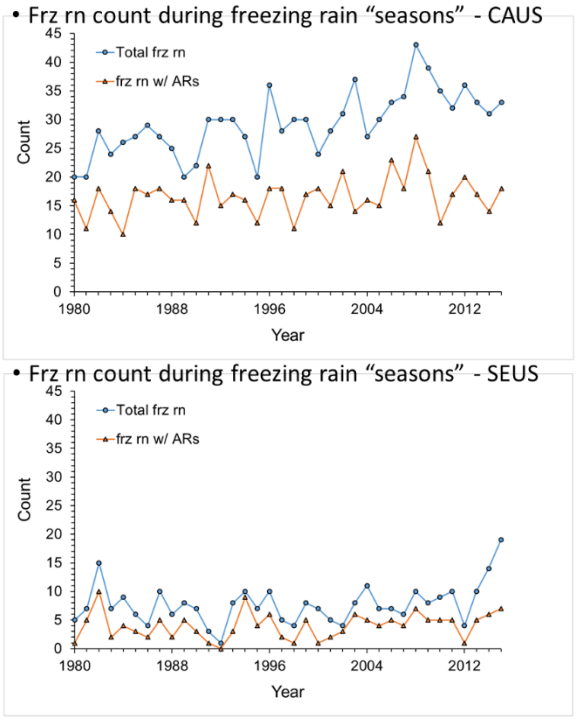

Figure 6. LD freezing rain event counts for the northern (CAUS, upper) and southern (SEUS, lower) domains over the 36-year study period. All LD events are plotted in blue, while only those events influenced by ARs are plotted in orange.

station reports over the event duration (labeled 'Score' in Table 3), we find a listing that we assume to be strongly correlated with event severity. The top score of all events (upper portion of Table 3) occurred in the northern domain (CAUS) in January 1998, an event that has been the focus of many studies (e.g., Gyakum 2016) as it was an extraordinarily damaging and deadly event.

CAUS	Frz rn (count)	(%)	Frz rn (h)	(%)
w/ AR	598	56.7	18168	65.4
total	1055		27768	

SEUS	Frz rn (count)	(%)	Frz rn (h)	(%)
w/ AR	135	48.4	3378	50.9
total	279		6636	

Table 1. Overall counts for AR-influenced and total LD freezing rain events of the northern (CAUS, upper) and southern (SEUS, lower) domains over the 36-year study period.

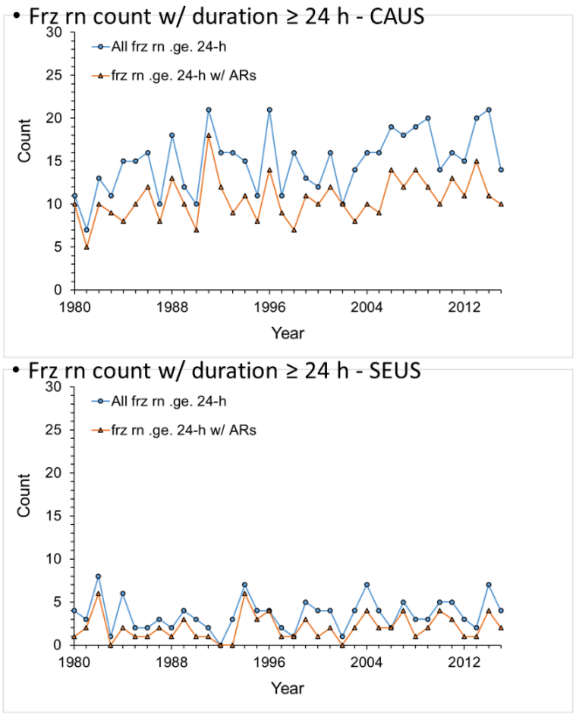

Figure 7. As in Figure 6, except for LD freezing rain events of at least 24-h duration (defined as 'VERY LONG' LD freezing rain events in the text).

Of note is that 14 of 15 of the top-ranked events in both domains is AR-influenced (column #4 of Table 3). The category (final column of Table 3) corresponds to populations in which LD freezing rain events occurred in the labeled study domain only ('o') or LD freezing rain events that occurred in the primary (labeled) domain, but also consisted of reports of freezing rain in the other domain ('+'). Examination of individual event duration in both domains (column #2 of Table 3) shows that ALL top events were VERY LONG LD freezing rain events, with a duration range of 36-180 h in the northern domain and 36-90 h in the southern domain.

CAUS	Frz rn (count)	(%)	Frz rn (h)	(%)
w/ AR	382	71.0	14976	73.5
total	538	(56.7)	20370	(65.4)

SEUS	Frz rn (count)	(%)	Frz rn (h)	(%)
w/ AR	74	57.4	2490	56.0
total	129	(48.4)	4446	(50.9)

Table 2. As in Table 1, except for LD freezing rain events of at least 24-h duration (defined as 'VERY LONG' LD freezing rain events in the text).

Start	Duration (h)	Score	AR-influenced	Category
1998 1 3 6	180	262	Y	CAUSo
1999 112 6	102	188	Y	CAUS+
1990 21312	96	170	Y	CAUSo
1989 3 4 0	72	138	Y	CAUS+
2011 2 1 0	60	134	Y	CAUS+
20131220 0	102	129	Y	CAUSo
2002123018	114	125	N	CAUSo
1995 227 0	54	124	Y	CAUS+
1995 111 6	108	119	Y	CAUS+
2009 1 612	42	119	Y	CAUS+
2008 3 3 0	78	111	Y	CAUSo
1991 3 3 0	60	110	Y	CAUSo
1986 21618	84	107	Y	CAUSo
1994 12718	36	103	Y	CAUS+
19831212 0	90	101	Y	CAUSo

Start	Duration (h)	Score	AR-influenced	Category
1994 2 812	90	207	Y	SEUS+
2004 12512	66	139	Y	SEUS+
1998122312	78	108	Y	SEUSo
19891218 0	54	97	Y	SEUSo
2000 129 0	54	95	Y	SEUS+
2014 211 6	72	94	Y	SEUS+
2011 110 0	72	93	Y	SEUSo
1982 11218	60	91	Y	SEUSo
2005 129 0	48	77	Y	SEUSo
1996 2 2 0	42	72	Y	SEUSo
1983 12012	78	71	Y	SEUS+
200212 412	36	68	N	SEUSo
1985 2 5 6	36	59	Y	SEUSo
2003 21518	48	58	Y	SEUS+
1994 127 0	42	55	Y	SEUS+

Table 3. Top 15 extreme (2.5%) LD freezing rain events of the northern (CAUS, upper) and strong (5.0%) LD freezing rain events of the southern (SEUS, lower) domains over the 36-year study period.

For those most severe LD freezing rain events having an AR influence listed in Table 3, an examination of AR characteristics and composite mean and anomaly patterns of the four basic populations (CAUSo, CAUS+, SEUSo, SEUS+) might prove insightful in identifying important characteristics that could be exploited by forecasters to warn of potentially severe freezing rain events.

Several parameters are available for inspection in the Guan and Waliser (2015) CFSR-based AR database. Mean zonal and meridional components of the IVT vector for every AR associated with events falling in the extreme or strong LD freezing rain events was compared to those components of ARs associated with 'normal' (event score near the median; in the 8-10 range) to investigate differences having statistical significance. A box and whisker plot of the mean IVT components is provided in Figure 8 and illustrates a single population that differs from five of the others ($p < 0.01$). Mean zonal IVT for AR-influenced LD freezing rain events in the strong SEUSo population was significantly greater than the mean zonal IVT

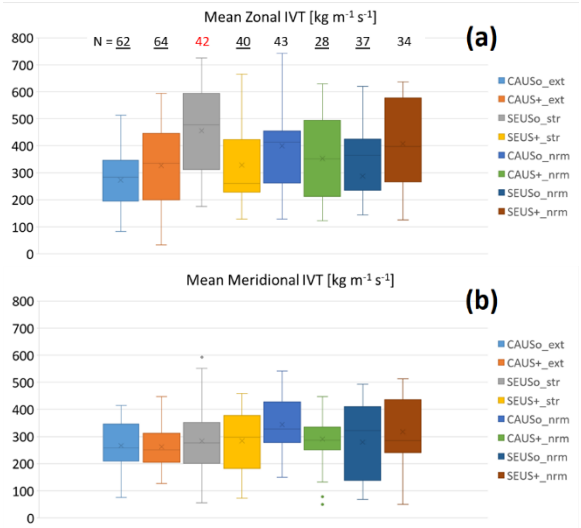

Figure 8. AR mean (a) zonal and (b) meridional IVT characteristics for the top 15 extreme LD freezing rain CAUS events (first set of two boxes), strong LD freezing rain SEUS events (second set of two boxes), normal LD freezing rain CAUS events (third set of two boxes), and normal LD freezing rain SEUS events (fourth set of two boxes). In each two box set, the first represents AR-influenced LD freezing rain events occurred in the appropriate study domain only ('o') and the second represents AR-influenced LD freezing rain events that occurred in the primary (labeled) domain, but also had reports of freezing rain in the other domain ('+'). The numbers in panel (a) represent the AR sample size of each domain/event intensity population. Only one population (SEUSo, red font) was found to have a statistically significant difference in mean zonal IVT compared to five other populations (boldface and underlined).

component of five other samples (extreme CAUSo, and CAUS+, strong SEUS+, and normal CAUS+ and SEUSo).

The reason for this significant difference is seen when comparing the composite means of the 500 hPa level geopotential heights of the extreme CAUS and strong SEUS events plotted in Figure 9. A strong gradient in geopotential height over the SEUS domain suggests the presence of a jet core having significant zonal flow. The corresponding anomaly map (Figure 10) shows the 'only' events (CAUSo and SEUSo) dominated by high amplitude and long wavelength anomalies, compared to the 'plus' events (CAUS+ and SEUS+). The dominant SEUSo composite anomaly corresponds to a trough west of the domain, while the dominant NEUSo composite anomaly corresponds to a ridge located offshore of the east coast. The amplitude and wavelength of these anomalies are suggestive of particularly long duration (slow moving) events.

Examination of composite means of the 850 hPa level geopotential height (Figure 11) shows a difference in

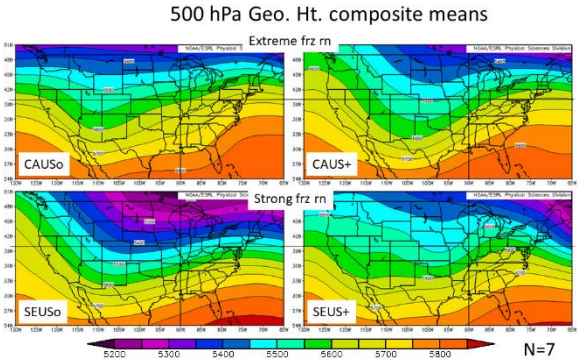

Figure 9. Composite mean 500 hPa level geopotential height (m) for (upper left) CAUSo, (upper right) CAUS+, (lower left) SEUSo, and (lower right) SEUS+ AR-influenced LD freezing rain events. The upper panels consist of the top 14 extreme (2.5%) CAUS LD freezing rain events and the lower panels consist of the strong (5.0%) SEUS LD freezing rain events. The left-hand column represents LD freezing rain event populations in which AR-influenced LD freezing rain events occurred in the labeled study domain only ('o') and the right-hand column represents AR-influenced LD freezing rain events that occurred in the primary (labeled) domain, but also had reports of freezing rain in the other domain ('+') Thin vertical line corresponds to 90º West longitude and thin horizontal line corresponds to 40º North latitude, the border between the CAUS and SEUS domains. Each panel is a composite of seven events (figures courtesy of ESRL | Physical Sciences Division).

mean trough orientation between the CAUS+ and SEUS+ composites. The resulting orientation of composite mean geopotential gradient is directed toward the southeast in the CAUS+ composite compared to a more easterly direction in the SEUS+ composite, implying more southwesterly flow in the CAUS+ events (assuming winds are close to geostrophic) and more southerly flow during the SEUS+ events. The corresponding composite mean (Figure 12) and anomaly (Figure 13) maps of the 850 hPa level temperature show the primary determinant of the 'only' events. The mid-level warm layer is clearly visible in the CAUSo maps, capable of

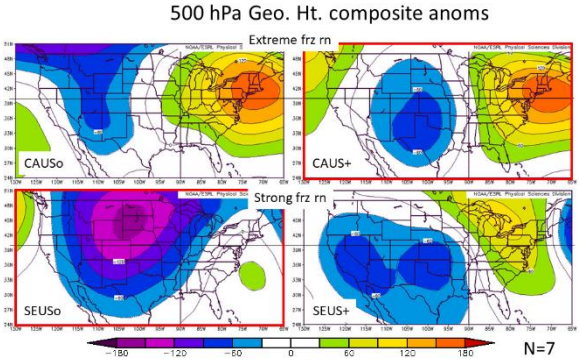

Figure 10. As in Fig. 9, except composite anomaly 500 hPa level geopotential height (m).

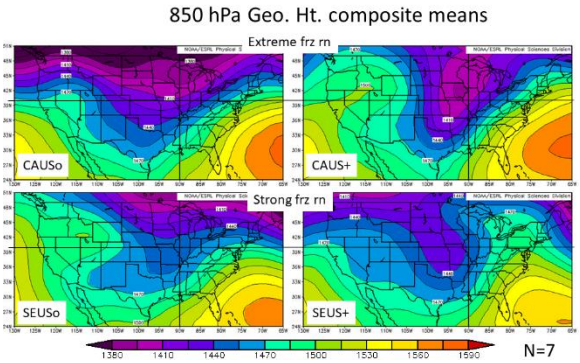

Figure 11. As in Fig. 9, except composite mean 850 hPa level geopotential height (m).

maintaining a LD freezing rain event. The transport of warm and humid air to the northern domain makes the air too warm to initiate or sustain any freezing rain in the southern domain. The opposite is true of the CAUSo population, transport of the shallow layer of cold air next to the surface is strong enough to reach the southern domain, but the absence of a mid-level layer of warm air in the northern domain makes the initiation and sustenance of freezing rain impossible. Hence, the SEUS domain is experiencing rain during the CAUSo extreme events and the CAUS domain is experiencing snow during the strong SEUSo events.

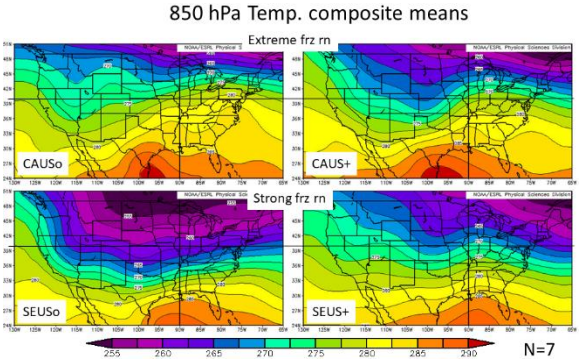

Figure 12. As in Fig. 9, except composite mean 850 hPa level temperature (K).

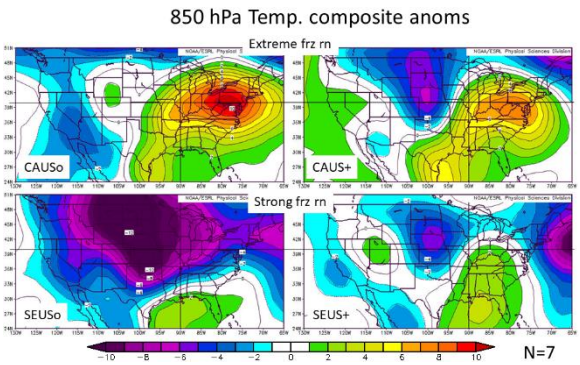

Figure 13. As in Fig. 9, except composite anomaly 850 hPa level temperature (K).

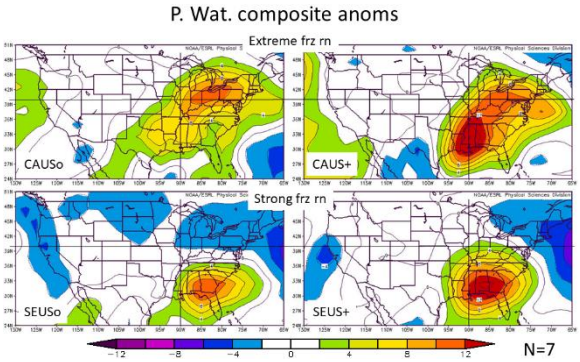

Figure 14. As in Fig. 9, except composite anomaly precipitable water (kg m^{-2}).

Composite anomalies of precipitable water (PW, Figure 14) shows strong anomalies for the 'plus' (CAUS+ and SEUS+) events whose centers are located in the deep south of the U.S. The slight positional differences of the two 'plus' domain PW anomalies show them to be located in the ideal upstream position for maximizing water vapor transport into the appropriate domains (see previous Fig. 11 discussion). In contrast, PW anomalies in the 'only' event composites is weaker and quite isolated for the SEUSo composite. This is consistent with what was discussed previously concerning the presence of the jet core overhead the SEUSo domain.

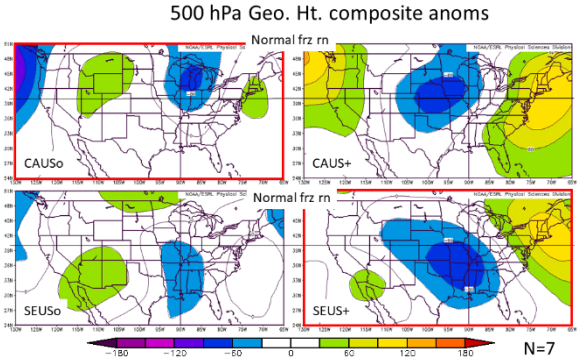

Figure 15. As in Fig. 10, except for populations having normal LD freezing rain events.

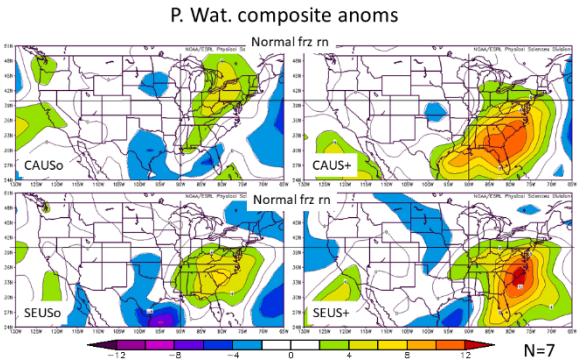

Figure 16. As in Fig. 14, except for populations having normal LD freezing rain events.

A comparison of composite anomalies of the normal (close to the median) LD freezing rain event samples of the 500 hPa level geopotential height (Figure 15) and precipitable water (Figure 16) can illustrate systematic differences in the events by utilizing contributions of the dynamic and thermodynamic terms of Eq. (1) and implications for their differences as presented in the Figure 2 discussion. It is assumed that PW anomalies serve as a proxy for lower tropospheric equivalent potential temperature, an indicator of maritime tropical air mass intensity.

The dynamic contribution to composite precipitation accumulation is examined by comparing composite anomalies of the 500 hPa level geopotential height (Figures 10 and 15). The amplitude and wavelength of the CAUSo and SEUSo anomalies is much smaller for the normal LD events (Figure 15; UL and LL), implying these events are associated with shortwaves (more progressive and of relatively shorter duration). The position of the normal SEUS+ anomaly (Figure 15; LR) is shifted significantly eastward compared to that of the strong anomaly. The orientation of the normal CAUS+ anomaly (Figure 15; UR) is rotated to having a more positive tilt, implying a progressive large-scale pattern. Red outlines on the borders of the CAUS+ and SEUSo panels in Figure 10 and of the CAUSo and SEUS+ panels in Figure 15 indicate those samples having a higher magnitude 850 hPa level vertical motion (not shown). Based on the influence of the dynamic term alone [Eq. (1)], the normal events of CAUSo and SEUS+ would be expected to produce more severe LD freezing rain events.

The thermodynamic contribution to composite precipitation accumulation is examined by comparing composite PW anomalies (Figures 14 and 16). Examination of all four samples of the normal events (Figure 16) shows PW anomalies consistently lower, indicative of a significantly less intense maritime tropical air mass overhead of the two study domains. The only substantial PW anomaly maximum of the normal events is associated with SEUS+, but is shifted substantially eastward, a less-than-optimal position for contributing toward high intensity precipitation in the SEUS study domain. The PW anomaly associated with normal CAUS+ events is also shifted too far eastward to contribute to intense precipitation in the northern domain.

4. SUMMARY AND CONCLUSIONS

ARs transport water vapor for LD freezing rain events ranging from extreme and strong to normal severity. With the exception of SEUSo events, mean AR characteristics are indistinguishable between events of extreme to lesser severity. Hence, examination of the synoptic pattern is important for identifying severe events from those having a lesser impact.

Extreme CAUSo and strong SEUSo events are associated with high amplitude, long wavelength synoptic patterns. The strong anticyclonic (cyclonic) 500 hPa level geopotential height anomaly of the CAUSo (SEUSo) composite highlights a pattern responsible for a mid-level warm (low-level cold) layer in the northern (southern) domain of sufficient strength to initiate and maintain VERY LONG LD freezing rain events.

A comparison of composites of extreme and strong LD (severe) freezing rain events of the CAUS and SEUS domains, respectively, to normal LD (non-severe) freezing rain events of both domains indicates that events of the latter category are incapable of producing severe events for several reasons. Intensity of the maritime tropical air mass of the normal events is weak either because horizontal transport of water vapor is diminished or the moisture ridge is located too far downstream of the forecast domain. A strong dynamic contribution in CAUSo and SEUS+ normal events is incapable of overcoming the weak thermodynamic contribution to create intense precipitation. These shortcomings, coupled with their relatively short durations (CAUS; 12-30 h, SEUS; 12-36 h), make event total accumulated precipitation for normal LD freezing rain events rather unspectacular.

5. REFERENCES

Doswell, C. A., H. E. Brooks, and R. A. Maddox, 1996: Flash flood forecasting: An ingredients-based methodology. *Wea. Forecasting*, **11**, 560-580.

Guan, B., and D. E. Waliser, 2015: Detection of atmospheric rivers: Evaluation and application of an algorithm for global studies, *J. Geophys. Res. Atmos*., **120, 12,** 514–12, 535, doi:10.1002/2015JD024257

Gyakum, J. R., 2008: The application of Fred Sanders' teaching to current research on extreme cold-season precipitation events in the Saint Lawrence River Valley region. *Synoptic-Dynamic Meteorology and Weather Analysis and Forecasting, A Tribute to Fred Sanders.* Lance F. Bosart and Howard B. Bluestein, Eds. Amer. Meteor. Soc., 241-250.

Gyakum, J. R., A. Wood, E. Atallah, S. Millrad, 2016: Atmospheric Rivers over eastern Canada: Their seasonality, impact on air mass dynamics, and links to extreme precipitation. *2016 International Atmospheric Rivers Conference*, San Diego, CA.

McCray, C., Atallah, E., Gyakum, J., 2019: Long-duration freezing rain events over North America: Regional climatology and thermodynamic evolution. *Wea. Forecasting*, **34**, 665–681. https://doi.org/10.1175/WAF-D-18-0154.1

Miller, D. K., D. Hotz, J. Winton, L. Stewart, 2018: Investigation of atmospheric rivers impacting the Pigeon River Basin of the southern Appalachian Mountains. *Wea. Forecasting*, **33**, 283–299, https://doi.org/10.1175/WAF-D-17-0060.1.